Investigation of the Radiative Forcings of Thin Cirrus in the Tropical Atmosphere Using AIRS/ARM Data

Qing Yue, K. N. Liou, and Y. Gu
University of California, Los Angeles, Los Angeles, California

Introduction and Motivation

• Cirrus clouds are the highest clouds in the troposphere, regularly cover 20–30% of the globe (Liou 1986) and have been found to have a high frequency of occurrence (e. g. Wylie et al. 2004).

• Given the high location, large coverage, and frequent occurrence, the effect of cirrus clouds on the energy balance of the earth-atmosphere system is a critically important research topic.

• The Fu-Liou (1993, Fu 1996, Fu et al. 1998) parameterization of cirrus clouds radiative properties has been upgraded by using a model of mixed ice crystal habits. Sensitivity studies has been carried out to study the effect of ice crystal size and shape on cirrus cloud radiative forcing.

• Using AIRS data, a thin cirrus retrieval scheme has been developed (Yue et al. 2006) and applied to a number of nighttime ARM-TWP scenes to determine cirrus optical depth and ice crystal size and shapes.

• Infrared radiative flux and heating rates in nighttime cirrus cloudy atmospheres have been computed using the improved Fu-Liou radiative transfer scheme.

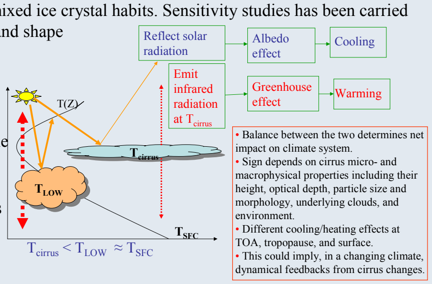

Methodology

The AIRS-retrieved optical depth, particle size, and ice water content of the thin cirrus clouds (Yue et al. 2006), and the atmospheric profiles measured by AIRS.

US Standard Atmosphere, and a cirrus layer located between 9.5 and 10.5 km at different *IWC* and D_e.

A: New parameterization
• Light scattering data calculated by unified theory
• mixed habits*

B: Experimental parameterization
• Light scattering data same as A
• Single habit assumption as in C

C: Previous parameterization (Fu and Liou 1993, Fu 1996, Fu et al. 1998)
• Light scattering data calculated by ray tracing programs for hexagonal crystals.
• Single habit: columns and plates with minimum ice crystal size larger than 20 µm.

Heating rate and cirrus cloud radiative forcings of the selected AIRS pixels

Sensitivity studies showing the size and shape effects on ice cloud radiative forcings

* • Tropics: 33.7% 41.6% 24.7%

* • Midlatitudes:
$L > 70$ µm 30% 30% 20% 20%
$L < 70$ µm 50% 25% 25%

Summary

➢ A new parameterization of the radiative properties of cirrus clouds for use in the Fu-Liou radiative transfer program has been developed. Non-spherical habits in addition to columns and plates are accounted for in this parameterization.

➢ Three sensitivity experiments have been carried out to study the size and shape effects of ice crystals on the broadband radiative properties, heating rates, and cloud radiative forcings of cirrus cloud. Results show that 1)smaller particles could reflect more solar radiation and trap more IR radiation for given ice water content; 2) compared with columns, the mixed habits will result in an increase of solar reflection and decrease of trapped infrared radiation at the TOA; 3) the new parameterization by a model of mixed habits and use of new light scatting database could produce a stronger solar albedo effect and weaker infrared greenhouse effect.

➢ Using the retrieved cirrus properties from AIRS data and the new parameterization, we find that infrared cloud forcing generally increases as ice water content and particle size increase. The modeled and infrared fluxes at the surface are compared correspondingly with ARM radiometric observations. For thin cirrus located near the tropical tropopause, the infrared cloud radiative forcings can be over 100 and 7 W/m² at the tropical tropopause and the surface, respectively. Other factors, such as water vapor and cloud position, also affect cloud radiative forcings and require further study.

➢ Daytime cases are needed to study the solar and net radiative forcing of these thin cirrus cases. A larger tropical cirrus database would be required to further understand radiative impacts of thin cirrus.

Sensitivity Study: Size and Shape Effect on Cloud Radiative Forcing (CRF)

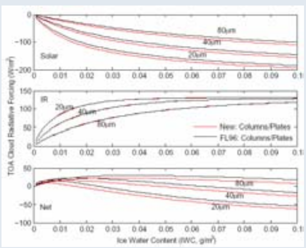

Ice cloud radiative forcings calculated by Parameterization B and C: same habit assumption, different light scattering database.

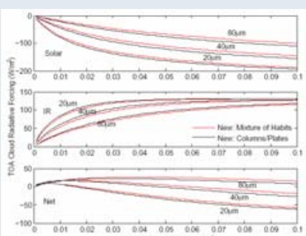

Ice cloud radiative forcings calculated by Parameterization A and B: same light scattering database, single habit VS mixed habits.

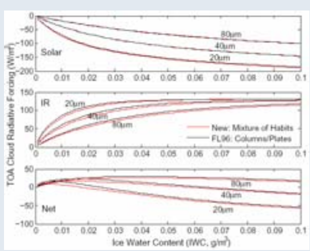

Ice cloud radiative forcings calculated by new parameterization A and original Fu-Liou Parameterization C

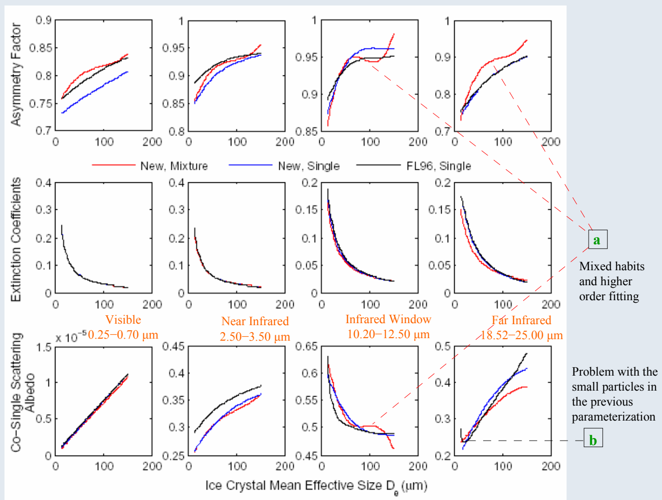

Asymmetry factor, extinction coefficient, and co-single scattering albedo as a function of ice crystal mean effective size calculated according to three different parameterization coefficients (Red: A; blue: B; black: C)

$$D_e = 1.5\,V/A \cong 1.2990\,D_{ge}$$

• For hexagonal particles, the effective particle size of a cloud layer defined in the new parameterization, D_e, can be related to the "generalized effective size", D_{ge}, used in the previous Fu-Liou parameterization as shown by equation above, which was generalized to apply to other shapes in our study for comparison purpose.

• The broadband asymmetry factor g, extinction coefficient β, and co-single scattering albedo $1-\omega$, parameterized as a function of D_e, are shown in four Fu-Liou bands. Both the change of light scattering database and the habit distribution will affect the calculation of broadband radiative properties, fluxes, and heating rates. As an example, we analyze the asymmetry factor g.

1. The use of new database results in a smaller g in the solar bands which increases solar reflection, while in the infrared bands, g is larger than the original except in the longest wavelength. However, the magnitude of this change is only half of that in the solar bands, which explains the small difference in the infrared CRF.
2. A model of mixed habits results in a larger g (smaller CRF) in the solar bands, and a smaller g in the mid-infrared region than the single habit scheme. However, g in the far infrared and 11 µm bands becomes significantly larger for the mixed habits scheme which causes a smaller infrared CRF.
3. Using new database and mixed habits of ice crystals, g calculated by the new parameterization is generally larger in the infrared bands than that by the original Fu-Liou parameterization, which results in less trapped infrared radiation at TOA. In the solar region, g by the new parameterization scheme is larger than the original one in the visible band, however, this relation is reversed as wavelength increases, therefore, the solar CRF calculated using the new scheme increases less than 10 w/m² even at high *IWC* when D_e=20 µm.

Case Study, Validation, and Discussions

I: Retrieval of the Thin Cirrus Cloud Properties and Validation by ARM MMCR and MPL Data.

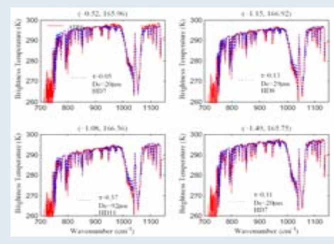

Thin cirrus BT spectra for four AIRS pixels in Granule 2005.03.01.147. The cloud properties were determined by a χ^2-minimization method.

• Two AIRS granules were selected: Granule 159 on 2003.06.20 over Manus Island, and Granule 147 on 2005.03.01 over Nauru Island, in which 14 and 15 pixels with thin cirrus cloud were selected around ARM TWP sites at Manus Island and Nauru Island, respectively.

• Computed and observed AIRS spectra agree very well for pixels with small optical depths.

• Largest residuals occur in the ozone band.

• The thin cirrus retrieval results were validated using ARM MMCR and MPL measurement (Yue et al. 2006). Only eight pixels are available by applying a collocation method.

2003.06.20.159 Pixels		4	8	10	14
τ	MMCR	0.07	0.03	0.13	~0
	AIRS	0.2	0.09	0.26	0.01
D_e (µm)	MMCR	81	87	106	~0
	AIRS	78	67	91.5	19.6

The AIRS-inferred optical depths (ice crystal sizes) are larger (smaller) than MMCR-retrieved values, possibly due to MMCR's missing small particles (Comstock et al. 2002), thus underestimating extinction coefficient.

2005.03.01.147 Pixels		6	9	10	13
AIRS	D_e (µm)	20	29	92	20
	τ	.05	.13	.37	.11
MPL	τ	.02	.15	.17	.10

Pixel 6 corresponds with the thin and high cirrus layer missed by MMCR. Pixel 9 is closest to the ARM site. Pixel 10 and 13 corresponds to thicker cirrus clouds, which MPL did not have backscattering after 19UTC. Therefore, 1-hour average MPL retrieval for these two pixels is smaller than AIRS retrieved optical depth.

II: Broadband Radiative Transfer Calculation and Comparison with ARM Radiometer Measurements.

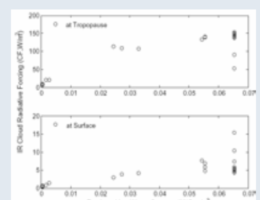

Calculated cirrus infrared radiative forcings for the 29 selected pixels as a function of retrieved ice water content.

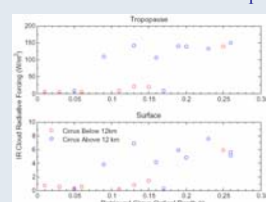

Calculated infrared CRF for the 29 selected AIRS pixels as a function of retrieved cirrus cloud optical depth. Red circles correspond with warmer cirrus clouds which are below 12 km, while blue ones are colder cirrus clouds located above 12 km.

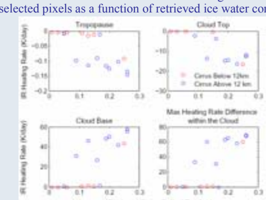

Calculated cirrus infrared heating rates at different levels of the atmosphere for the 29 selected pixels as a function of retrieved cirrus optical depth.

• Generally, the magnitude of the CRF in the infrared region increase as *IWC* increases despite clouds form under different environment conditions. There is a similar pattern for D_e (not shown).

• CRF due to thin cirrus show strong dependence on the cloud position. For cirrus with optical depths smaller than 0.3, the infrared CRF increase as τ increases in given cloud position range.

• Although cirrus is very thin, infrared CRF at tropopause and surface can be over 100 and 7 W/m², respectively, due to the high position of the cirrus cloud.

• The collocation method was applied to the ARM radiometer data time series. One hour average was taken for the fluxes observed by ARM program.

• ARM radiometer measurements are 1-min data from the pyrgeometer, which is located four meters above the mean sea level at Manus Island site, and 7 meters at Nauru Island site.

• The surface infrared fluxes calculated by our model are larger than the ARM radiometer measurements, which is probably due to the absorption of the tropical atmosphere layer between the location of the instrument and sea surface.

2003.06.20.159 Pixels		4	8	10	14
$F^{\uparrow}_{sfc}$(IR) (w/m²)	ARM	452.9	454.5	443.9	449.3
	Model	457.2	468.2	474.0	472.1
$F^{\downarrow}_{sfc}$(IR) (w/m²)	ARM	401.7	410.0	402.6	406.8
	Model	406.1	410.0	412.9	403.1

2005.03.01.147 Pixels		6	9	10	13
$F^{\uparrow}_{sfc}$(IR) (w/m²)	ARM	458.2	457.3	457.0	461.1
	Model	473.2	469.6	476.4	468.5
$F^{\downarrow}_{sfc}$(IR) (w/m²)	ARM	418.9	418.9	415.5	433.0
	Model	424.3	424.3	436.4	422.9

Corresponding author address: Qing Yue, Department of Atmospheric and Oceanic sciences, University of California, Los Angeles, 405 Hilgard Ave., Los Angeles, CA, 90095–1565, E-mail: qingyue@atmos.ucla.edu